## LITERATURE CITED

Campbell, J. A., "The Velocity-Concentration Relationship in Mass Transfer to a Wall," Ph.D. Thesis, University of Illinois, Urbana (1981).

Campbell, J. A., and T. J. Hanratty, "Mass Transfer Between a Turbulent Fluid and a Solid Boundary: Linear Theory," *AIChE J.*, p. 988 (Nov., 1982).

Fortuna, G., and T. J. Hanratty, "The Influence of Drag-reducing Polymers on Turbulence in the Viscous Sublayer," *J. Fluid Mech.*, **53**, 575 (1972).

Hogenes, J. H. A., "Identification of the Dominant Flow Structure in the Viscous Wall Region of a Turbulent Flow," Ph.D. Thesis, University of Illinois, Urbana (1979).

Lee, M. K., L. D. Eckelman, and T. J. Hanratty, "Identification of Turbulent Wall Eddies Through the Phase Relation of the Components of the Fluctuating Velocity Gradient," *J. Fluid Mech.*, **66**, 17 (1974).

Mitchell, J. E., and T. J. Hanratty, "A Study of Turbulence at a Wall Using an Electrochemical Wall-Stress Meter," *J. Fluid Mech.*, **26**, 199 (1966).

Reiss, L. P., "Investigation of Turbulence Near a Pipe Wall Using a Diffusion Controlled Electrolytic Reaction on a Circular Electrode," Ph.D. Thesis, University of Illinois, Urbana (1967).

Reiss, L. P., and T. J. Hanratty, "Measurement of Instantaneous Rates of Mass Transfer to a Small Sink on a Wall," *AIChE J.*, **8**, 245 (1962).

Reiss, L. P., and T. J. Hanratty, "An Experimental Study of the Unsteady Nature of the Viscous Sublayer," *AIChE J.*, **9**, 154 (1963).

Sirkar, K. K., "Turbulence in the Immediate Vicinity of a Wall and Fully Developed Mass Transfer at High Schmidt Numbers," Ph.D. Thesis, University of Illinois, Urbana (1969).

Sirkar, K. K. and T. J. Hanratty, "The Limiting Behavior of the Turbulent Transverse Velocity Component Close to a Wall," *J. Fluid Mech.*, **44**, 605 (1970).

Shaw, D. A., and T. J. Hanratty, "Influence of Schmidt Number on the Fluctuations of Turbulent Mass Transfer to a Wall," *AIChE J.*, **23**, 160 (1977a).

Shaw, D. A., and T. J. Hanratty, "Turbulent Mass Transfer Rates to a Wall for Large Schmidt Numbers," *AIChE J.*, **23**, 28 (1977b).

Van Shaw, P., and T. J. Hanratty, "Fluctuations in the Local Rate of Turbulent Mass Transfer to a Pipe Wall," *AIChE J.*, **10**, 475 (1964).

Welch, P. D., "The Use of Fast Fourier Transform for the Estimation of Power Spectra: A Method Based on Time Averaging Over Short, Modified Periodograms," *IEEE Trans. on Audio and Electroacoustics*, **15**, 70 (1967).



*Manuscript received July 10, 1981; revision received April 2, and accepted April 19, 1982.*


# Mechanism of Turbulent Mass Transfer at a Solid Boundary


**Mass transfer between a turbulent fluid and a solid boundary is considered for the case of large Schmidt numbers. The variation of the mass transfer coefficient with time, $K(t)$, is calculated by solving the mass balance equation using a random velocity input. An interpretation of the mass transfer process which is radically different from that given by classical approaches is obtained.**



**J. A. CAMPBELL and T. J. HANRATTY**

**University of Illinois**
**Urbana, IL 61801**


## SCOPE

The goal of a theory of turbulent mass transfer is to relate the mass transfer rate at a solid boundary to measurable properties of the fluctuating velocity field. For large Schmidt numbers, this is simplified because the concentration boundary layer is so thin that only the limiting behavior of the velocity field close to the solid surface needs to be considered. Solutions of a linearized form of the mass balance equations (Campbell and Hanratty, 1981a) have suggested a theory which is quite different from classical approaches. It shows that the mass transfer boundary layer acts as a filter in that only low frequency velocity fluctuations containing a small fraction of the turbulent energy are controlling the mass transfer process. However, this interpretation is open to question, since a number of the results obtained from the linear theory analysis are not satisfactory. The calculated dependency of the mass transfer coefficient on Schmidt number, $\overline{K} \sim S^{-3/4}$, does not agree with experiment and calculated intensities of the mass transfer fluctuations are much too high. In the research described in this paper, numerical solutions of nonlinear forms of the mass balance equations were carried out using a random input for the velocity field. The results of this calculation appear as a randomly varying mass transfer coefficient, $K(t)$, and a randomly varying concentration field, $C(y,t)$. The statistical properties of these results can then be compared with experiment.

Two types of nonlinear model equations were explored. In one of these, only normal velocity fluctuations, $v(y,t) = \beta(t)y^2$, are considered. In the other, the influence of the transverse velocity fluctuations is included by using a velocity field which is periodic in the transverse direction.

## CONCLUSIONS AND SIGNIFICANCE

The results of these calculations confirm the picture of turbulent mass transfer at a solid boundary presented by the solutions of the linear mass balance equations. Only velocity fluctuations of low frequency are influencing the mass transfer rate. There is no observable difference betwee mass transfer rates calculated from a velocity input containing a spectrum of frequencies and those calculated from a velocity input containing only low frequencies (Figure 5).

There are, however, interesting differences between the linear and nonlinear calculations. For the linear case, the frequency


0001-1541-83-6672-0221-$2.00. © The American Institute of Chemical Engineers, 1983.

**of the velocity fluctuations controlling turbulent mass transfer is approximately the same at all $y$ and concentration profiles calculated for different Schmidt numbers can be plotted in a similarity form if $y$ is normalized with $\delta_c \sim S^{-1/4}$. For the nonlinear case, it is found that high frequency velocity fluctuations play a more important role with increasing $y$. Because of this, the variation of the average concentration with distance from the wall cannot be characterized by a single length parameter and the calculated Schmidt number dependency, $\overline{K} \sim S^{-0.7}$, is much closer to experiment.**

**The property of the velocity field that has been found to be of critical importance in predicting mass transfer rates is the limiting value of the spectral density function of $\beta$ for small frequency, $W_\beta(0)$. It is suggested that this be determined from measurements of the spectral density function of the mass transfer fluctuations (Eq. 10). An equation for $\overline{K}$ of the following form is obtained from the nonlinear calculations:**

$$\overline{K} = 0.09 \left( \frac{W_\beta(0)}{0.01} \right)^{0.21} S^{-0.7}.$$

## INTRODUCTION

Mass transfer between a turbulently flowing fluid and a solid boundary at large Schmidt number, $S$, is characterized by a concentration boundary layer which is thinner than the viscous sublayer region, where the variation of average velocity, $\overline{U}(y)$, is given by the equation for rectilinear laminar motion. Consequently the velocity field within the boundary layer is given by the first term in a Taylor series expansion in distance from the wall. For a fully developed velocity field,

$$U = \overline{U}(y) + \alpha(x,z,t)y, \tag{1}$$

$$v = \beta(x,z,t)y^2, \tag{2}$$

$$w = \gamma(x,z,t)y, \tag{3}$$

where $U$ is the velocity in the streamwise direction, $v$, normal to the wall and $w$, in the transverse direction. From conservation of mass, the following relation among $\beta$, $\alpha$ and $\gamma$ is obtained:

$$2\beta = -\frac{\partial \alpha}{\partial x} - \frac{\partial \gamma}{\partial z}. \tag{4}$$

The rate of mass transfer per unit area between a turbulent fluid and a solid boundary, $N$, is usually characterized by a mass transfer coefficient, $K$, defined by:

$$N = K(C_B - C_W), \tag{5}$$

where $C_B$ is the bulk concentration and $C_W$ is the concentration at the solid boundary. The goal of a theory for turbulent mass transfer is to relate statistical properties of $K$ to statistical properties of $\alpha$, $\beta$ and $\gamma$.

The development of such a theory has been of interest to this laboratory for a number of years. In these researches, electrochemical techniques have been used to study $\alpha$ and $\gamma$ (Reiss, 1962; Fortuna, 1970; Eckelman, 1971; Lau, 1980; Hogenes, 1979; Sirkar, 1969) and to study the local time averaged, $\overline{K}$, and the local fluctuation in the mass transfer coefficient, $k = K - \overline{K}$ (Shaw, 1976; Sirkar, 1969; Van Shaw, 1963). These researches have revealed that scales in the streamwise and transverse directions characterizing $k$ are similar to those found for $\alpha$ and $\gamma$ but that the frequency of $k(t)$ is much smaller. An increase in the Schmidt number causes the characteristic frequency of $k$ to decrease.

A solution of a form of the mass balance equation linear in the fluctuations by Campbell and Hanratty (1981a) has provided a possible interpretation of these results and a theory for mass transfer to a solid boundary which is quite different from classical approaches to this problem. It is suggested by linear theory that at large $S$ the mass transfer process is not controlled by the most energetic velocity fluctuations. The concentration boundary layer acts as a filter in that only low frequency velocity fluctuations are effective in causing concentration fluctuations. Lower and lower fractions of the turbulent energy are used in transporting mass as the Schmidt number increases.

Calculations based on linear theory, however, do not predict the correct magnitudes of, nor the correct influence of Schmidt number on, $\overline{K}$ and $\overline{k^2}/\overline{K}^2$. In order to give stronger support to the proposed theory, it was necessary for us to carry out solutions of a nonlinear form of the mass balance equation. The results of this effort are reported in this paper.

The first use of the nonlinear mass balance equation to predict mass transfer at a wall was presented by Brodkey et al. (1978). They ignored the influence of the transverse and streamwise velocity fluctuations and modeled the normal velocity fluctuations by a signal which changed its magnitude discontinuously at dimensionless time intervals of $\Delta t = 8.0$. The magnitude of $v$ at the beginning of a time interval was determined by using a Gaussian random number generator. The change of the magnitude of $(\overline{v^2})^{1/2}$ with distance from the wall, $y$, was obtained from a fit to experimental data which gave a linear variation at small $y$.

Campbell and Hanratty (1979) solved the nonlinear mass balance equation using the velocity field obtained from the model of a typical wall eddy explored by Hatziavramidis and Hanratty (1979). In this work, the velocity is assumed to be varying periodically in time and in $z$. The perioid was chosen to be the bursting period.

Predictions of mass transfer rates based on the calculations of Brodkey et al. (1978) and by Campbell and Hanratty (1979) do not agree with experiment. The reason for this is that unrealistic spatial and time variations are assumed for the velocity field.

In this paper velocity fields are used which contain a spectrum of frequencies. The time variation of the velocity is obtained from experimental measurements, the spatial variations, by modeling assumptions. Two models are used. In one, the effect of transverse velocities is ignored, $\gamma = 0$. In the other, the influence of transverse velocities is included by assuming a spatial variation of $\gamma$ which is characterized by a single harmonic.

Of particular interest are the calculations in which the normal velocity is low pass filtered. These enabled us to examine directly that the removal of the most energetic velocity fluctuations does not influence mass transfer at large Schmidt numbers. The results of the first model support the interpretation provided by linear theory and give the correct dependency of $\overline{K}$ and $\overline{k^2}/\overline{K}^2$ on Schmidt number. The inclusion of the transverse velocities improves the accuracy of the calculations of the concentration profile and also shows a spatial variation of the mass transfer coefficient which is consistent with what is observed in experiments.

Of particular importance to these calculations are the results of an analysis of experimental measurements of $\gamma(z,t)$ that have been low pass filtered (Campbell and Hanratty, 1981b). These reveal that the low frequency velocity fluctuations have approximately the same transverse scale as the most energetic velocity fluctuations. We used this information to specify the scale of the transverse velocities in the second model.

## THEORY

### (a) Simplified Mass Balance Equation

Experimental measurements show that the concentration field

is approximately homogeneous in the flow direction and that concentration variations in the $y$-direction are more rapid than in the $z$-direction. Order of magnitude arguments of the type presented by Sirkar and Hanratty (1970), can be used to develop the following simplified form of the mass balance equation for fully developed flows at large Schmidt numbers, $S$:

$$\frac{\partial C}{\partial t} + v\frac{\partial C}{\partial y} + w\frac{\partial C}{\partial z} = \frac{1}{S}\frac{\partial^2 C}{\partial y^2}, \tag{6}$$

where $C$ is the concentration relative to that at the wall. All terms in Eq. 6 have been made dimensionless using the concentration difference, $C_B - C_W$, the friction velocity, $u^*$, and the kinematic viscosity, $\nu$.

Equation 6 is to be solved using the boundary conditions $C = 0$ at $y = 0$ and $C = 1$ at large $y$.

#### (b) Linear Equation

The following equation for the concentration fluctuations,

$$c = C - \overline{C}, \tag{7}$$

is obtained if terms nonlinear in the fluctuating quantities are ignored (Campbell and Hanratty, 1981a):

$$\frac{\partial c}{\partial t} + \beta y^2\frac{d\overline{C}}{dy} = \frac{1}{S}\frac{\partial^2 c}{\partial y^2}. \tag{8}$$

This has been solved for the case of $c = 0$ at $y = 0$ and at large $y$. Solutions of the equation have been presented by Sirkar and Hanratty (1970) and by Campbell and Hanratty (1981a). Of particular interest for the work presented in this paper is the result obtained for high frequency.

A spectral function for $\beta$, $W_\beta(n)$, can be defined which has the property

$$\overline{\beta^2} = \int_0^\infty W_\beta(n)\, dn, \tag{9}$$

where $n$ is the frequency in cycles per second made dimensionless using $u^*$ and $\nu$. For large $n$ linear theory gives the following relation between the spectral density functions for $\beta$ and $k$:

$$W_k(n) = W_\beta(n)\frac{\overline{K}^2 4}{(2\pi n)^3 S}. \tag{10}$$

At high $S$ the spectral function for $k$ is confined to a region where $W_\beta(n)$ is approximately constant (Figure 1) so that

$$W_\beta(n) = W_\beta(0). \tag{11}$$

The linear analysis presented by Campbell and Hanratty (1981a), as well as the calculations described in this paper, show that $W_\beta(0)$ is of central importance in characterizing turbulent mass transfer to a solid boundary. Consequently, the result (Eq. 10) is of considerable interest since it provides a means to measure $W_\beta(0)$. One of the important goals of the work reported here is to see whether nonlinear models give Eq. 10 at high frequencies.

#### (c) Nonlinear Model I

Our initial efforts in solving Eq. 6 were to ignore the influence of transverse velocities. Then Eq. 6 reduces to the model equation explored by Brodkey et al. (1978):

$$\frac{\partial C}{\partial t} + \beta(t) y^2\frac{\partial C}{\partial y} = \frac{1}{S}\frac{\partial^2 C}{\partial y^2}. \tag{12}$$

This is to be solved using prescribed values of $\beta(t)$ at a fixed location at the wall.

A theoretical problem in using Eq. 12 is that it appears to violate the law of conservation of mass since $\partial v/\partial y \neq 0$. However, this is not the case since velocity fluctuations parallel to the wall are not assumed to be zero. What is implied by Eq. 12 is that variations of the concentration field parallel to the wall can always be neglected compared to concentration variations perpendicular to the wall, i.e., $\partial C/\partial z$, $\partial C/\partial x \cong 0$. This difficulty can be overcome by using a model which includes effects of mixing in planes parallel to the wall.

#### (d) Nonlinear Model II

If only mixing in the transverse direction is added to Eq. 12, the following equation explored by Campbell and Hanratty (1979), is obtained:

$$\frac{\partial C}{\partial t} + \beta(z,t) y^2\frac{\partial C}{\partial y} + \gamma(z,t) y\frac{\partial C}{\partial z} = \frac{1}{S}\left[\frac{\partial^2 C}{\partial y^2} + \frac{\partial^2 C}{\partial z^2}\right] \tag{13}$$

Insufficient experimental information is presently available to completely specify $\beta(z,t)$ and $\gamma(z,t)$. Therefore a simplified model was used.

It is assumed that transverse mixing occurs principally through velocity fluctuations which are approximately homogeneous in the flow direction and which have a transverse wavelength of $\lambda$. From the results presented in the paper by Campbell and Hanratty (1981b), we select $\lambda \cong 60$–$100$. The following equations are obtained for $\beta(z,t)$ and $\gamma(z,t)$:

$$\beta(z,t) = (2)^{1/2}\beta(t)\cos(2\pi z/\lambda) \tag{14}$$

$$\gamma(z,t) = -(2)^{1/2}\beta(t)\frac{\lambda}{2\pi}\sin(2\pi z/\lambda). \tag{15}$$

Here $\beta(t)$ is the specified time variation of $\beta$ at a given location on the boundary. The factor $(2)^{1/2}$ is included so that the mean-squared value of $\beta$, obtained by averaging Eq. 14 both in time and in space, is equal to $\overline{\beta^2(t)}$.

As discussed by Campbell (1981), significant contributions to $\beta$ are made by disturbances with smaller transverse scales than $\lambda = 60$–$100$ and perhaps by disturbances in the streamwise direction. Consequently, we have also explored models in which only a fraction, $f$, of the energy of $\beta(t)$ is associated with streamwise wall eddies. Results obtained from these calculations are not strongly dependent on the selection of a value for $f$. Consequently, for simplicity, we present results only for $f = 1$ in this paper.

## SPECIFICATION OF $\beta(t)$

A method for approximating $\beta(t)$ is suggested from conservation of mass, Eq. 4. If the velocity is assumed to be homogeneous in the flow direction,

$$\beta \cong -\tfrac{1}{2}\frac{\partial \gamma}{\partial z}. \tag{16}$$

The derivative $\partial\gamma/\partial z$ can be determined if measurements can be made of $\gamma$ at fixed $x$ but at a small distance $\Delta z$ apart.

$$\beta \cong -\tfrac{1}{2}\frac{\Delta \gamma}{\Delta z}. \tag{17}$$

The method for measuring $\gamma$ is described in a previous paper by Campbell and Hanratty (1981b). The term $\beta(t)$ was evaluated from Eq. 17 using measurements at $\Delta z = 10.8$ and 4.9.

The measurements of $(\overline{\beta^2})^{1/2}$ appear to be about $\frac{1}{3}$ to $\frac{1}{4}$ of what would be suggested by extrapolating the measurements of $(\overline{v^2})^{1/2}$ of Eckelmann (1974) and of Laufer (1953) to $y \to 0$. Furthermore the value of $W_\beta$ measured for $n \to 0$ is lower than what is calculated by Shaw and Hanratty (1977) from Eq. 10 and their measurements of $W_k(n)$.

It is our feeling that the most reliable method for determining $W_\beta(0)$ is through measurements of $W_k(n)$. Therefore we concluded that the measurement method outlined above produced too small a value of $\beta(t)$. The reason for this is that it ignored small scale fluctuations of $u$ in the $x$-direction and of $w$ in the $z$-direction, which, apparently, are making large contributions to $\beta(t)$. (For a detailed discussion of this matter, see the thesis by Campbell, 1981.) Consequently, we multiplied the measurements of $\beta(t)$ by a factor of $F \cong 2.4$,

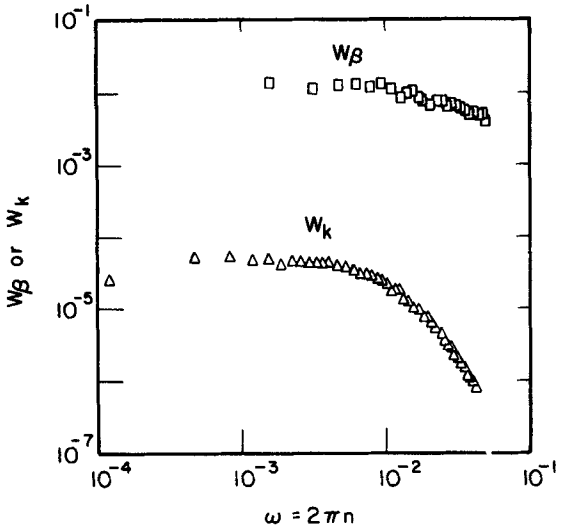


**Figure 1. Spectral density functions for $\beta$ and $k$ from experimental measurements.**

$$\beta \cong -\tfrac{1}{2} F \frac{\Delta\gamma}{\Delta z}, \tag{18}$$

selected so that $W_\beta(0) = 0.01$, to be consistent with the value determined from the spectral function $W_k(n)$ at large $n$.

The function $\beta(t)$ used in our calculations, is, therefore, a random signal characterized by a variance of

$$\overline{\beta^2} = (0.008)^2 \tag{19}$$

and by the spectral density function shown in Figure 1. For comparison, the spectral density function of $k$ at a Schmidt number of 695 is also presented.

## NUMERICAL METHODS

The one-dimensional and the two-dimensional mass balance equations, (Eqs. 12 and 13), were solved with finite difference techniques which involved upwinding of the velocity terms (Roache, 1972). A digitalized record of the measurements of $\beta(t)$ described in the previous section of this paper was used in calculation of the velocity fields (Eq. 2, or Eqs. 14 and 15). The digital data extended over a real time period of 4,000 s and contained 10,000 points ($\Delta t = 10$). Since the results were sensitive only to the low frequency part of the velocity signal, the spectral density function for the signal may be considered constant, equal to $W_\beta(0)$. Consequently, the calculations could probably have been carried out with any signal which could be characterized as white noise.

The numerical solution of the one-dimensional mass balance equation used an implicit method. The two-dimensional equation was solved using an alternating-direction implicit method (Campbell, 1979). The boundary conditions at the well-mixed boundary were $dC/dy = 0$ for outflows and $C = 1$ for inflows. The zero gradient outer boundary condition was picked so diffusion at the outer boundary would be negligible for outflows.

In solving Eq. 12, upwind differencing approximates $v\,\partial C/\partial y$ for outflows as $v_j(C_j - C_{j-1})/\Delta y$. This can be written as

$$v_j(C_j - C_{j-1})/\Delta y = (v_jC_j - v_{j-1}C_{j-1})/\Delta y + (v_j - v_{j-1})C_{j-1} \tag{20}$$

The first term on the right side of Eq. 2 represents the net convection of mass out of the volume due to flow normal to the wall. From conservation of mass considerations $(v_j - v_{j-1})$ is balanced by an influx of material in a plane parallel to the wall. Therefore, Eq. 2 indicates that the finite difference form used for $v\,\partial C/\partial y$ for outflows pictures the flow in the plane parallel to the wall as carrying fluid of concentration $C_{j-1}$ into the volume element.

Similarly, for inflows the upwinding approximation gives the convective term as $v_j(C_{j+1} - C_j)/\Delta y$. From the above arguments we see that this finite difference form for inflows pictures flow parallel to the wall carrying fluid of concentration $C_{j+1}$ out of the volume element.

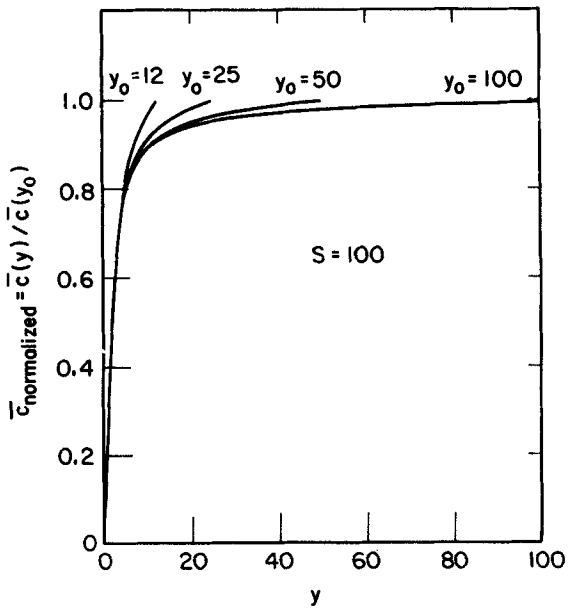


**Figure 2. Concentration profiles calculated from the 1-D nonlinear equation at various values of $y$.**

A consequence of the upwinding approximation for the one-dimensional model is that fixing the concentration at some outer boundary has no influence on the calculations during outflows. For sustained outflows low concentration fluid will extend to large values of $y$. The solution of the 1-D equation with a reasonable location for the outer boundary, therefore, results in an average concentration profile that does not reach 1 at large values of $y$. This problem is not encountered in the solution of the 2-D equation because the transverse mixing terms are modeled more accurately. The concentration profiles obtained from the 1-D study were all normalized equal to 1 at large $y$ so that the behavior at small $y$ could be compared with results that use the more realistic well mixed outer boundary.

The 1-D equation was solved using 10,000 time steps and 100 grid points in the normal direction. The 2-D equation used 1,000 to 2,000 time steps, and 30 grid points in the normal direction and 26 in the transverse direction. The consistency of the finite difference schemes was tested by varying the number of gridpoints in time and space and by varying the initial conditions.

The concentration profiles at large $y$ calculated from the 1-D equation, were found to be sensitive to the choice of $y_o$. This is illustrated in Figure 2 where concentration profiles for a Schmidt number of 100 are plotted for values of $y_o$ of 12, 25, 50, and 100. It is to be noted that the concentration field, and, therefore, the calculated $\overline{K}$, at small $y$ is independent of $y_o$. It appears that if a large enough value of $y_o$ were used an asymptote would be reached. The result, however, would have little meaning, for at values of $y$ greater than 7 the concentration profile is no longer within the viscous sublayer.

Calculations of the concentration profile for the 2-D model at a Schmidt number of 1,000 for values of $y_o$ equal to 3, 5, 10, 20 are presented in Figure 61 of the thesis by Campbell (1981). Again these show no effect of the choice of $y_o$ on the calculation of $\overline{K}$. There is an effect on the values of $\overline{C}$ calculated for large values of $y$, but not so severe as for the 1-D model. For example, no significant difference was obtained with the calculations using $y_o = 10$ and $y_o = 20$.

## RESULTS OF NONLINEAR MODEL I

### (a) Calculations of $K(t)$

A comparison of the calculated $k(t)$ with the input signal $\beta(t)$

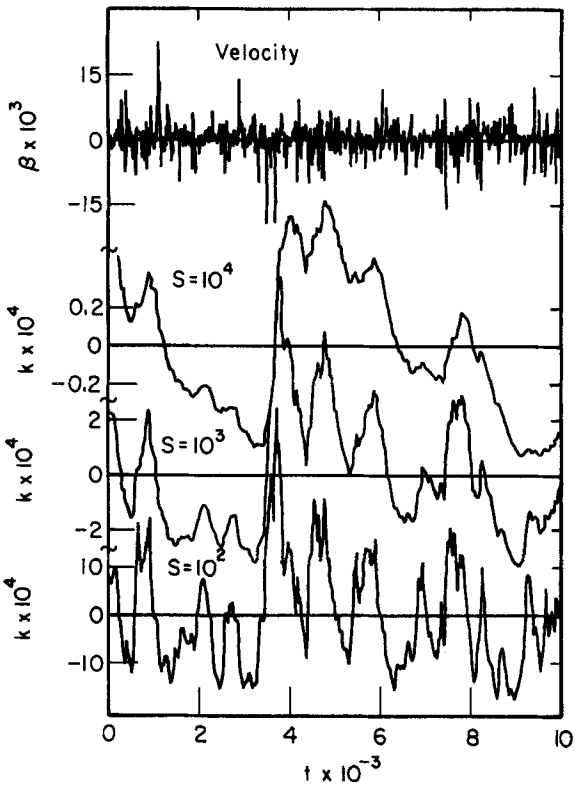


Figure 3. Comparison of velocity input and mass transfer output from 1-D nonlinear equation at $S$ = 100, 1,000, 10,000.

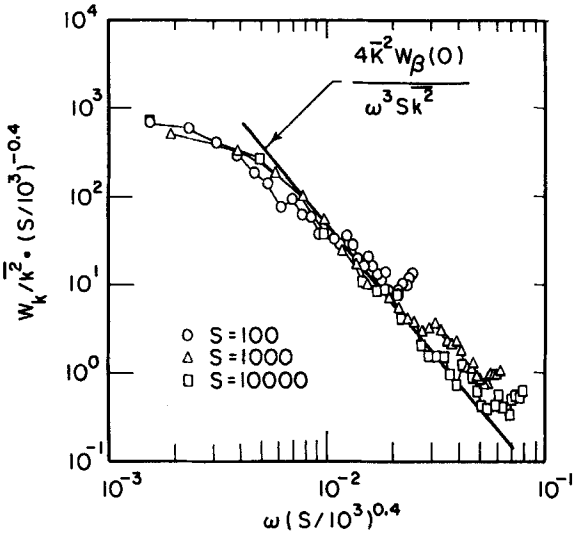


Figure 4. Mass transfer spectra from 1-D nonlinear equations plotted with proper scaling.

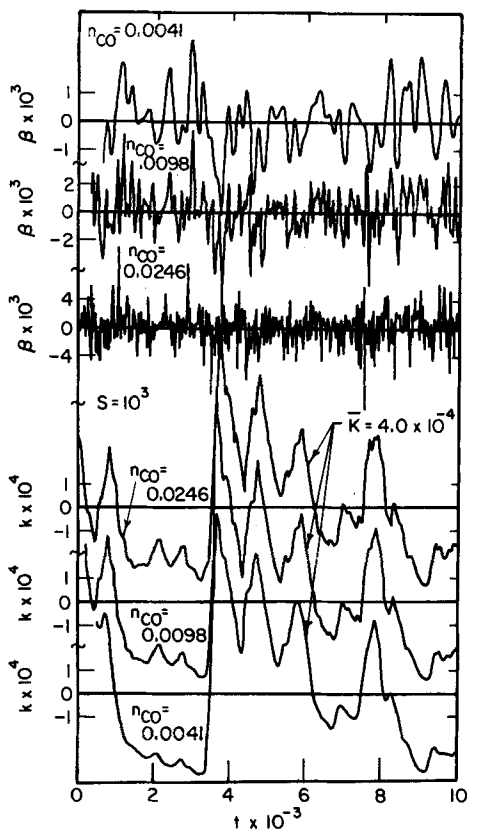


Figure 5. The time variation of the mass transfer coefficient obtained with the input velocity low pass filtered at different values of $n_{co}$. (1-D model)

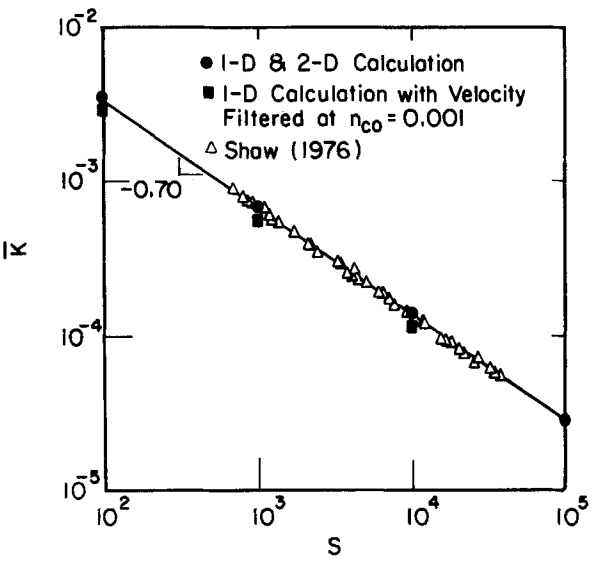


Figure 6. Average mass transfer coefficient vs. Schmidt number from 1-D and 2-D nonlinear equations.

using nonlinear model I is shown in Figure 3 for three different Schmidt numbers. The effect of Schmidt number in damping high frequency fluctuations is clearly indicated.

The spectral functions are shown in Figure 4, where the ordinate and abscissa have been normalized with Schmidt number in the manner suggested by Shaw and Hanratty to collapse the data onto a single curve. Of particular interest is the agreement of the calculations with Eq. 10 at large frequencies. This supports the suggestion that measurements of $W_k(n)$ provides a method for measuring $W_\beta(0)$.

Calculations of $K(t)$ using $\beta(t)$ signals that had been low pass filtered at different cut-off frequencies, $n_{co}$, are shown in Figure 5. A comparison of the upper signals shows strong changes in the velocity signal by filtering at $n_{co}$ = 0.0246 and at $n_{co}$ = 0.0098 (80% of the energy removed). It is noted, however, that no discernible effect is found in the calculated $K(t)$ (lower signals). If the velocity signal is filtered so that 95% of the energy has been removed ($n_{co}$ = 0.0041, changes in the calculated $K(t)$ can be detected but the overall shape of the relation remains the same. These calculations clearly show that only the low frequency velocity fluctuations in the region where $W_\beta(n) = W_\beta(0)$ are determining $\overline{K}$ and $K(t)$ at high Schmidt numbers.

The calculated influence of $S$ on $\overline{K}$ shown in Figure 6 is in close agreement with the experimental results of Shaw and Hanratty (1977). It is found that $\overline{K} \sim S^{-0.70}$. The effect of filtering on the calculated $\overline{K}$ is also shown in Figure 6 for $n_{co}$ = 0.001 for which ~ 99% of the energy of the $\beta(t)$ signal was removed. It is noted that

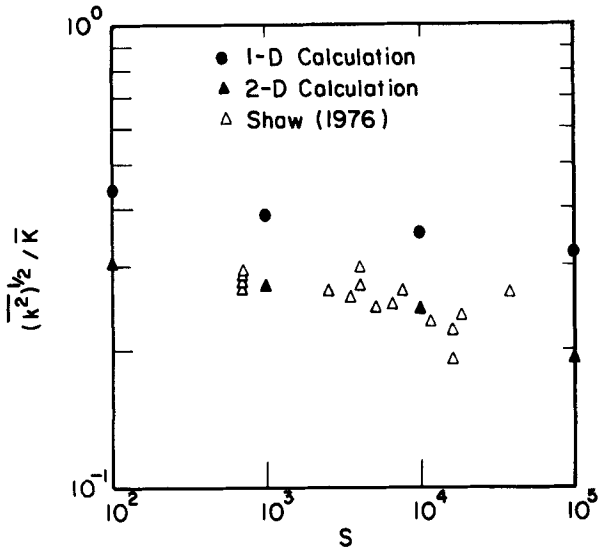


Figure 7. Relative intensity of the fluctuations of the mass transfer coefficient from nonlinear calculations.

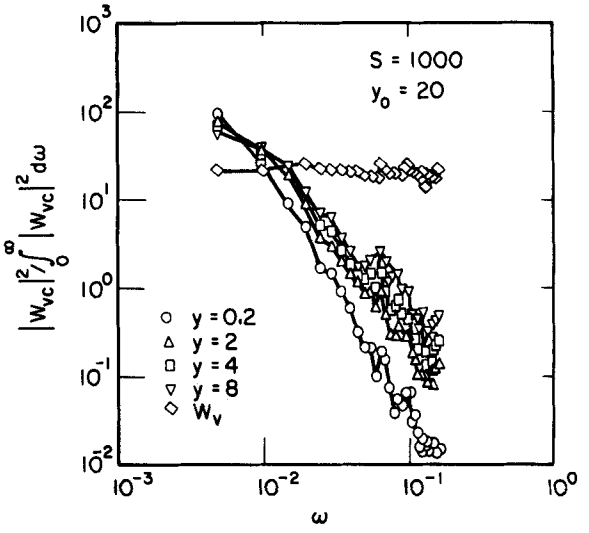


Figure 9. Cross-spectra of *vc* at several values of *y* from 1-D nonlinear equation.

this causes only a 10% decrease in the calculated $\overline{K}$ at $S = 1000$.

The influence of $S$ on $(\overline{k^2})^{1/2}/\overline{K}$ is shown in Figure 7. Calculated intensities are found to decrease with Schmidt number as indicated by experimental measurements. The one-dimensional calculations are too high by a factor of 1.4.

### (b) Calculation of $c(y,t)$ and $C(y)$

Calculated examples of the time variation of $c$ at different values of $y$ are shown in Figure 8. For comparison, unfiltered and filtered velocity signals are shown over the same time interval. Of particular interest are the increase in the frequency content of the signal with increasing $y$ and the intermittancy at large values of $y$.

By comparing $c(t)$ at $y = 0.2$ with the velocity signal filtered at $n_{co} = 0.001$, one observes that the low frequency concentration fluctuations close to the wall are directly connected with low frequency velocity fluctuations. This can be seen by comparing the peaks in the concentration signal with inflows indicated by negative values of the filtered velocity signal.

It is observed that the quiescent periods in the $c(t)$ signal and the intervals of high frequency oscillations at large $y$ are respectively associated with low frequency inflows and outflows. An examination of the variation of the high frequency concentration fluctuations in the $y$-direction suggests that their scale is too large for molecular diffusion to be important so that $\partial C/\partial t \sim v\,\partial C/\partial y$. A low frequency inflow causes blunt shaped concentration profiles with very small values of $dC/dy$ at large $y$. A low frequency outflow causes diffuse concentration profiles with significant values of $dC/dy$ at large $y$. The above order of magnitude relation indicates large values of $\partial C/\partial t$ at large $y$ for outflows and, consequently, concentration fluctuations with frequencies comparable to the velocity fluctuations. The amplitude of these fluctuations increases with increasing distance from the wall since $v = \beta(t)y^2$. Consequently the high frequency concentration fluctuations arise

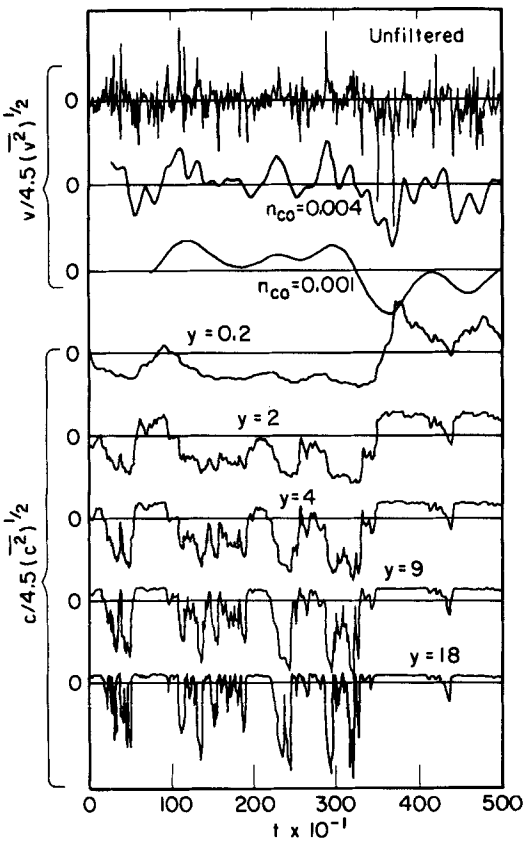


Figure 8. Concentration fluctuations at several values of *y* calculated from the 1-D equations at $S = 1{,}000$.

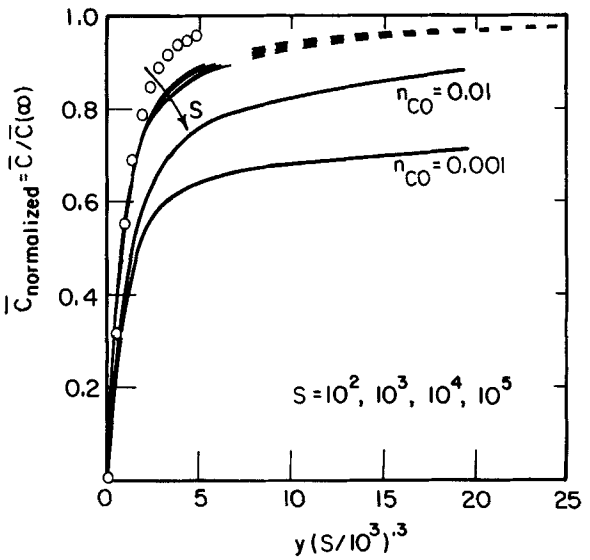


Figure 10. Concentration profiles calculated from the 1-D equation. The circles indicate data obtained by Lin et al. (1953), at $S = 900$.

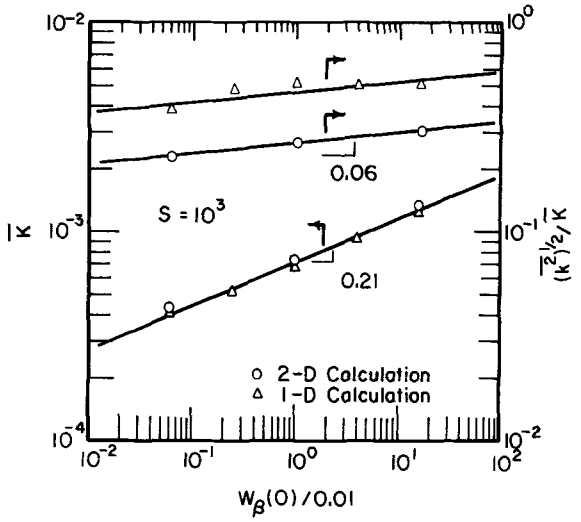


**Figure 11. The effect of $W_\beta(0)$ on the average mass transfer coefficient and the fluctuations in the mass transfer coefficient, obtained from the nonlinear calculations.**

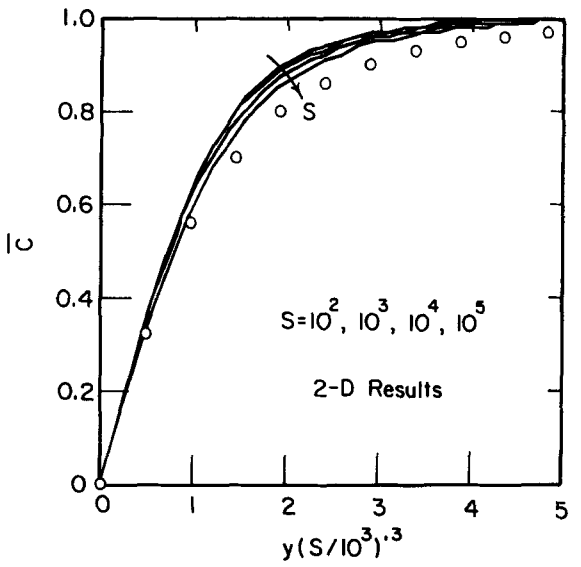


**Figure 12. Concentration profiles calculated from the 2-D equation. The circles indicate the data of Lin et al. (1953), at $S = 900$.**

because of a complex nonlinear interaction which causes them to ride on top of concentration waves associated with low frequency velocity fluctuations, containing only a small percent of the total turbulent energy.

The Reynolds transport has contributions from both of these modes throughout the concentration boundary layer. This is indicated in Figure 9, where spectra of $vc$ are plotted. It is noted that the frequency content of $vc$ increases with increasing $y$, but that its median frequency at all $y$ is much less than the median frequency of the velocity fluctuations.

The calculated average concentration is plotted as a function of distance from the wall in Figure 10. The abscissa has been normalized with $\delta_c = S^{-1}\overline{K}^{-1} = S^{-0.3}$, derived from the $\overline{K}$ vs. Schmidt number relation. It is observed that similarity is not obtained and that the scaling of the outer part of the concentration profile is different from that close to the wall. The influence of filtering on the concentration profile is also illustrated in Figure 10 where $\overline{C}(y)$ curves using a $\beta(t)$ signal with $n_{co} = 0.01$ and 0.001 are presented. This calculation clearly shows that high frequency velocity fluctuations are having a stronger effect on the variation of the concentration at distances farther from the wall.

### (c) Effect of $W_\beta(0)$

The mass transfer process at large Schmidt numbers is related to the velocity field primarily through the limiting value of the spectral density function of $\beta$ at small frequencies, $W_\beta(0)$. Calculations were carried out to explore the influence of variations of $W_\beta(0)$ by multiplying the $\beta(t)$ input by a constant factor. This had the effect of changing the magnitude of $W_\beta(0)$ while keeping the characteristic time the same; i.e., $W_\beta(0)/\overline{\beta^2}$ was held constant.

Plots of $\overline{K}$ and of $(\overline{k^2})^{1/2}/\overline{K}$ vs. $W_\beta(0)$ are presented in Figure 11 for a Schmidt number of 1,000. It is noted that the results for $\overline{K}$ and $(\overline{k^2})^{1/2}/\overline{K}$ are approximated by the relations

$$\overline{K} \sim S^{-0.70} W_\beta(0)^{0.21} \tag{21}$$

$$(\overline{k^2})^{1/2}/\overline{K} \sim S^{-0.06} W_\beta(0)^{0.06} \tag{22}$$

These are close to the $\overline{K} \sim [W_\beta(0)]^{1/4}$ and the $(\overline{k^2})^{1/2}/\overline{K} \sim [W_\beta(0)]^0$ relations for linear theory (Campbell and Hanratty, 1981a).

## RESULTS ON NONLINEAR MODEL II

An improvement in the calculated results can be obtained by including the effect of the convection term in the transverse direction through Eq. 13. This allows for a spatial variation of $K$ in the $z$-direction. More importantly, it gives additional mixing and a more realistic $\overline{C}$ at large $y$.

A transverse wavelength of $\lambda = 100$ was chosen for the velocity input because this is approximately equal to the value of the wavelengths of the velocity and the mass transfer observed experimentally. No effect on the average mass transfer rate or on the intensity of the mass transfer fluctuations was found when a wavelength of 50 was used.

As shown in Figure 6, values of $\overline{K}$ calculated from models I and II are equal. However, model II gives lower values of the fluctuations in $K$, in close agreement with experimental measurements (Figure 7).

Calculated variations of $\overline{C}$ vs. $y/\delta_c$ are given in Figure 12, with $\delta_c \sim S^{-0.3}$. It is seen that this scaling is valid only for small $y$ and that the larger the value of $S$, the smaller is the range over which it holds. A comparison with Figure 10 shows that the 2-D results are much less diffuse at large y than are the 1-D results. A comparison with the measurements of Lin et al. (1953) at $S = 900$ shows that the inclusion of spanwise mixing in the 2-D model provides a much more realistic calculation of $\overline{C}(y)$. However, the differences between the calculations and the measurements indicates that the 2-D model is not completely accurate in representing the mixing at large $y$.

As with the 1-D model, high frequency velocity fluctuations are found to assume an increased importance in transporting mass as $y$ increase. This is illustrated in Figure 13 where example calculations of $c(t)$ are presented over the same time interval used in Figure 8. A comparison of Figures 8 and 13 shows very similar qualitative behavior for the 1-D and 2-D calculations.

The 2-D model uses three hydrodynamic parameters

$$\overline{K} \sim (S, W_\beta(0), \overline{\beta^2}, \lambda). \tag{23}$$

However the insensitivity of the calculations to the selection of $\lambda$ and the close agreement between the values of $\overline{K}$ calculated by the 1-D and 2-D models, indicates that $\overline{K}$ is primarily dependent on $W_\beta(0)$. Calculations of the influence of $W_\beta(0)$ on values of $\overline{K}$ obtained from the 2-D calculations are given in Figure 11. It is noted that both the 1-D and 2-D models give essentially the same result so the same equation for $\overline{K}$ presented in the last section is again obtained,

$$\overline{K} = 0.09 \left[\frac{W_\beta(0)}{0.01}\right]^{0.21} S^{-0.7} \tag{24}$$

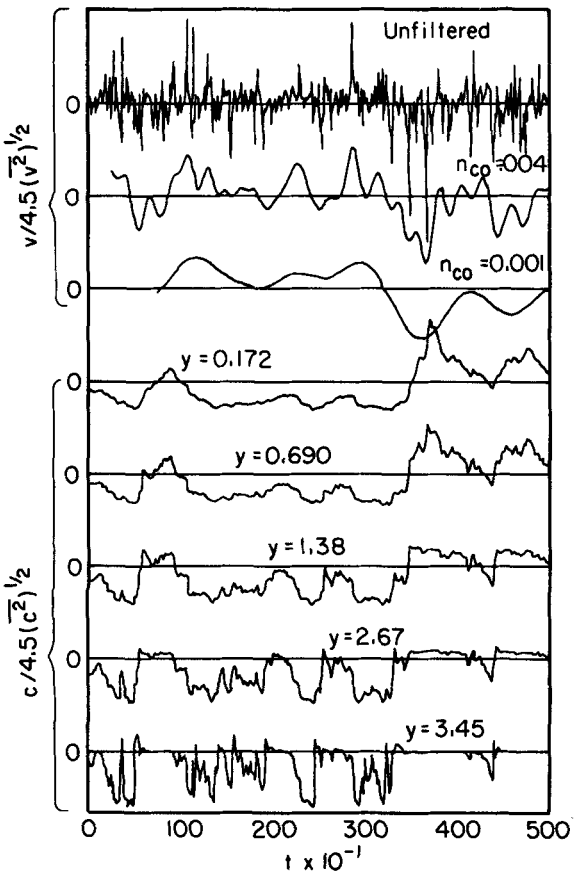


**Figure 13. Concentration fluctuations at several values of y calculated from the 2-D equation at $S = 1{,}000$, $z = 0$.**

## DISCUSSION

The nonlinear analysis presented in this paper supports a theory for turbulent mass transfer to a solid boundary which is radically different from classical approaches (surface renewal, Nernst diffusion layer, analogies, various eddy models). It views the concentration boundary layer as a filter which acts in such a way that low frequency velocity fluctuations, containing only a small fraction of the energy, are controlling the mass transfer rate.

We have identified the spectral density function of normal velocity fluctuations at small frequencies, $W_\beta(0)$, as being the property of the velocity field of critical importance. On the basis of numerical solutions of the 1-D and 2-D nonlinear mass balance equations, we suggest that Eq. 24 relates $\overline{K}$ to the turbulent velocity field. The parameter $W_\beta(0)$ is best determined from measurements of the spectral density function of the mass transfer fluctuations at large frequency through Eq. 10.

Solutions of the linear mass balance equations, discussed in a previous paper (Campbell and Hanratty, 1981a), give a similar picture. However, contrary to the results presented in this paper, the linear equations give $\overline{K} \sim S^{-3/4}$ and concentration profiles which scale with $\delta_c \sim S^{-0.25}$. The principle qualitative difference between the solutions of the linear and nonlinear equations is that the nonlinear results show that high frequency velocity fluctuations are playing a more important role in transporting mass at large $y$. (Compare Figure 9 with Figure 5 of the paper by Campbell and Hanratty, 1981a.) Traces of the temporal variation of the concentration for the nonlinear solutions show that high frequency concentration fluctuations ride on waves of low concentration caused by outward flows from the wall of very low frequency. We explain the need to use more than one length scale in interpreting the profiles of average concentration as being associated with the increasing importance of high frequency fluctuations in transporting mass at large distances from the wall.

The 1-D and 2-D nonlinear equations give quite different behaviors of $\overline{C}(y)$ at large $y$. It is of interest, therefore, that both give essentially the same relation for $\overline{K}$. Apparently, the calculation of $\overline{K}$ is somewhat insensitive of the method for modeling the mixing at large $y$, so long as it takes account of the increasing importance of high frequency velocity fluctuations with increasing $y$. The inclusion of transverse velocities in the 2-D model improves the prediction of $\overline{C}(y)$ and $(\overline{k^2})^{1/2}/\overline{K}$ over what would be obtained with the 1-D model. However, the use of a periodic function with a single harmonic to represent transverse variations of the velocity field is certainly an oversimplification. Additional calculations need to be carried out with more realistic velocity fields that reflect the randomness in space, as well as in time.

Until such results are available, it is difficult to interpret the differences between the profiles of average concentration calculated with the 2-D model and the experiment of Lin et al. (1953).


## ACKNOWLEDGMENT

This work is being supported by the National Science Foundation under Grant NSF CPE 79-20980.


## NOTATION

$c,C$ = fluctuating and total concentrations relative to that at the wall made dimensionless with $C_B - C_W$
$C_B$ = bulk concentration of specie (mol/cm$^3$)
$C_W$ = wall concentration of specie (mol/cm$^3$)
$f$ = fraction of the normal velocity due to variations in the transverse velocity
$F$ = factor used in Eq. 18
$k,K$ = fluctuating and total mass transfer coefficient made dimensionless with $u^*$ (except in Eq. 5)
$n$ = frequency in Hz made dimensionless with $u^*$ and $\nu$
$n_{co}$ = cut-off frequency used in low pass filtering
$N$ = rate of mass transfer (mol/cm$^2$·s)
$S$ = Schmidt number = $\nu/D$
$t$ = time made dimensionless with $u^*$ and $\nu$
$u,U$ = fluctuating the total steamwise velocities made dimensionless with $u^*$
$u^*$ = friction velocity (cm/s)
$v,V$ = fluctuating and total normal velocities made dimensionless with $u^*$
$w,W$ = fluctuating and total transverse velocities made dimensionless with $u^*$
$W_k(\omega)$ = spectrum of the fluctuations of $k$
$W_\beta(\omega)$ = spectrum of the fluctuations of $\beta$
$x$ = coordinate in steamwise direction made dimensionless with $u^*$ and $\nu$
$y$ = coordinate perpendicular to wall made dimensionless with $u^*$ and $\nu$
$z$ = coordinate transverse to flow made dimensionless with $u^*$ and $\nu$

### Greek Letters

$\alpha$ = time varying part of dimensionless steamwise velocity = $u/y$
$\beta$ = time varying part of dimensionless normal velocity = $v/y^2$
$\gamma$ = time varying part of dimensionless transverse velocity = $w/y$
$\delta_c$ = length scale characterizing the thickness of the concentration boundary layer made dimensionless with $u^*$ and $\nu$
$\lambda$ = wavelength of the spatial scale in the transverse direction made dimensionless with $u^*$ and $\nu$
$\nu$ = kinematic viscosity (cm$^2$/s)
$\tau$ = Eulerian time scale of the autocorrelation of $\beta$
$\omega$ = circular frequency made dimensionless with $u^*$ and $\nu$

## LITERATURE CITED

Brodkey, R. S., K. N. McKelvey, H. C. Hershey, and S. G. Nychas, "Mass Transfer at the Wall as a Result of Coherent Structures in a Turbulently Flowing Liquid," *Int. J. Heat Mass Transfer*, **21**, 593 (1978).

Campbell, J. A., "The Use of a Regular Eddy Model to Describe Turbulent Mass Transfer to a Wall," M.S. Thesis, University of Illinois, Urbana (1979).

Campbell, J. A., "The Velocity-Concentration Relationship in Turbulent Mass Transfer to a Wall," Ph.D. Thesis, University of Illinois, Urbana (1981).

Campbell, J. A., and T. J. Hanratty, "Influence of Turbulent Structure on Mass Transfer at a Solid Surface," Proceedings of 2nd Symposium on Turbulent Shear Flows, London (1979).

Campbell, J. A., and T. J. Hanratty "Mass Transfer Between a Turbulent Fluid and a Solid Boundary: Linear Theory," *AIChE J.*, p. 988 (Nov., 1982).

Campbell, J. A. and T. J. Hanratty, "Turbulent Velocity Fluctuations that Control Mass Transfer to a Solid Boundary," *AIChE J.*, (March, 1983).

Eckelman, L. D., "The Structure of Wall Turbulence and its Relation to Eddy Transport," Ph.D. Thesis, University of Illinois, Urbana (1971).

Eckelmann, H., "The Structure of the Viscous Sublayer and the Adjacent Wall Region in Turbulent Channel Flow," *J. Fluid Mech.*, **65**, 439 (1974).

Fortuna, G., "The Effect of Drag-Reducing Polymers on Flow Near a Wall," Ph.D. Thesis, University of Illinois, Urbana (1970).

Hatziavramidis, D. T., and T. J. Hanratty, "The Representation of the Viscous Wall Region by a Regular Eddy Pattern," *J. Fluid Mech.*, **95**, 655 (1979).

Hogenes, J. H. A., "Identification of the Dominant Flow Structure in the Viscous Wall Region of a Turbulent Flow," Ph.D. Thesis, University of Illinois, Urbana (1979).

Laufer, J., "The Structure of Turbulence in Fully Developed Pipe Flow," *NACA TN 2954* (1953).

Lin, C. S., R. W. Moulton, and G. L. Putnam, "Mass Transfer Between Solid Wall and Fluid Streams," *Ind. Eng. Chem.*, **45**, 636 (1953).

Reiss, L. P., "Investigation of Turbulence Near a Pipe Wall Using a Diffusion Controlled Electrolytic Reaction on a Circular Electrode," Ph.D. Thesis, University of Illinois, Urbana (1962).

Roache, P. J., "Computational Fluid Dynamics," Hermosa Publishers, Albuquerque, N.M. (1972).

Shaw, D. A., "Mechanism of Turbulent Mass Transfer to a Pipe Wall at High Schmidt Number," Ph.D. Thesis, University of Illinois, Urbana (1976).

Shaw, D. A. and T. J. Hanratty, "Influence of Schmidt Number on the Fluctuations of Turbulent Mass Transfer to a Wall," *AIChE J.*, **23**, 160 (1977).

Sirkar, K. K., "Turbulence in the Immediate Vicinity of a Wall and Fully Developed Mass Transfer at High Schmidt Numbers," Ph.D. Thesis, University of Illinois, Urbana (1969).

Sirkar, K. K. and T. J. Hanratty, "Relation of Turbulent Mass Transfer at High Schmidt Numbers to the Velocity Field," *J. Fluid Mech.*, **44**, 589 (1970).

Van Shaw, P., "A Study of the Fluctuations and the Time Average of the Rate of Turbulent Mass Transfer to a Pipe Wall," Ph.D. Thesis, University of Illinois, Urbana (1963).


*Manuscript received August 19, 1981; revision received April 7, and accepted April 19, 1982.*

# Experimental Measurements of the Effect of Viscosity on Drag for Liquid Drops

The drag coefficients of drops of various liquids falling in air were measured experimentally. The drag coefficient was linearly related to the viscosity in the Reynolds number and viscosity range measured. Measurements also suggested there is no difference between Newtonian and non-Newtonian liquids.

**P. H. GILLASPY and T. E. HOFFER**

**Atmospheric Sciences Center**
**Desert Research Institute**
**University of Nevada System**
**Reno, NV 89506**

## SCOPE

Calculating fall trajectories and transport properties between a drop and its medium depends on a knowledge of the drag forces acting on the liquid drop. It has been found that the Reynolds number ($Re$) is the primary parameter characterizing the forces acting (Stokes, 1851; Reynolds, 1883). In the Stokes flow regime ($Re < 1$), exact solution of the Navier-Stokes equation for a sphere yields an expression for drag in excellent agreement with measurements for spheres and liquid drops. In the intermediate range ($1 < Re < 500$), numerical solutions (Hamielec et al., 1967; LeClair et al., 1970) give drag coefficients with excellent experimental agreement. The range of higher $Re$ sees a whole host of experimental measurements for spheres and liquid drops with the main emphasis on water drops due to their relevance to atmospheric sciences. Although the manner in which the various forces act is well understood, previous studies have not been able to express quantitatively the effect of liquid viscosity or surface tension on the drag at higher $Re$.

In the analysis of experimentally measured drag coefficients reported in this paper, quantitative assessment of the role of liquid drop viscosity on the drag is presented. Non-Newtonian as well as Newtonian liquids were used to separate the possible effects of rheological properties.

## CONCLUSIONS AND SIGNIFICANCE

Experimental measurements have been reported that show qualitatively and quantitatively the effects of liquid viscosity on the drag of liquid drops falling through air. The quantitative effects of viscosity have been shown to be modeled by a function of the form

$$C_D = C_D(Re,\mu = \infty)\left[1 - B\frac{\mu_a}{\mu} f(Re)\right] \qquad (1)$$

Correspondence concerning this paper should be addressed to P. H. Gillaspy at NASA/MSFC, Space Sciences Laboratory, ES-83, Huntsville, AL 35812.

0001-1541-83-6815-0229-$2.00. © The American Institute of Chemical Engineers, 1983.